RSC Advances

ROYAL SOCIETY OF CHEMISTRY

www.rsc.org/advances

Journal Name

COMMUNICATION

Diethylamine gas sensor using V_2O_5-decorated α-Fe_2O_3 nanorods as sensing material

Received 00th January 20xx,
Accepted 00th January 20xx

DOI: 10.1039/x0xx00000x

www.rsc.org/

Haonan Zhang[a], Yazi Luo[a], Ming zhuo[a], Ting Yang[c], Jiaojiao Liang[c], Ming Zhang[c], Jianmin Ma[c], Huigao Duan[c], Qiuhong Li*[a, b]

V_2O_5-decorated α-Fe_2O_3 composite nanorods were synthesized successfully by electrospinning and environment-friendly soak-calcination method. The composite showed high selectivity and stability to diethylamine gas as well as ultra fast response times within 2 s to 100 ppm diethylamine gas.

Semiconductor oxides have attracted more and more attentions because of their promising applications in lithium-ion batteries, photocatalyst, and gas sensors.[1-3] With increasing concerns of air pollution, haze, noxious gas on human health and safety, highly available oxide semiconductor-type gas sensors have attracted considerable interest due to their significant resistance change upon exposure to detecting combustible, explosive and poisonous gases.[4,5] It is well known that high sensitivity, rapid response, and excellent selectivity are three of most important properties for semiconductor-type gas sensors.[6,7] At present, several methods have been used for improving sensing performance, including element doping, noble metal functionalization, and multi metal oxides formed heterostructure construction.[8-14] For semiconductor-type gas sensors, the detection of gas analytes often depends on monitoring the direct change in the resistance in adsorption of oxygen and desorption of analyte molecules on the surface.[15-17] Key factors to the performance of gas sensors include three aspects: the transducer function, the receptor function, and the sensitive utilization of surface particles.[18-20] Based on the above mechanism, we are devoted to designing a metal oxide gas sensing material with large specific surface area, good porosity and uniformity. Electrospinning (ES) has been proposed as a technique for the preparation of one-dimensional (1D) metal oxide based nanostructures which can provide a simple and versatile route to preparing 1D nanostructures with a large surface area to volume ratio, flexibility in surface functionalities, and heterostructures.[21, 22]

α-Fe_2O_3 (hematite), a classical n-type semiconductor (E_g = 2.1 eV), which is a stable, nontoxic, low-cost iron oxide under ambient conditions, is of great scientific and technological importance.[23] V_2O_5 is also an n-type semiconducting oxide whose resistance decreases when the V^{5+} species are reduced to V^{4+} during the interaction with reducing gases.[24] These transition metal oxides have been extensively investigated because of the unique electrical and catalytic properties. Sensitive materials incorporated with V_2O_5 can significantly enhance the sensitivity[25,26]. Diethylamine is colorless, strong alkali and corrosive liquid with volatile and flammable nature. Diethylamine gas is used in the manufacture of pharmaceuticals, pesticides, dyes, rubber vulcanization accelerator, textile auxiliaries and metal preservatives, emulsifying agent, inhibitor, etc. Diethylamine gas has strong excitant, which can stimulate eye, trachea, lung, skin, and excretory system. Meanwhile there is no report on diethylamine gas sensing as far as we know. However it is very meaningful for the detection of diethylamine gas in chemical plant, pharmacy workshop, dye workshop, etc. Inhalation of vapor or mist of diethylamine, which is strong alkali, excitant, corrosive and flammable with ammonia smell, can cause laryngeal edema, bronchitis, chemical pneumonia, and pulmonary edema. High concentrations of diethylamine may lead to death. In this work, we present an attempt to enhance the response of semiconductor oxide gas sensor to diethylamine gas by synthesizing V_2O_5-decorated α-Fe_2O_3 composite with novel morphology and structure. Materials with nanoscale and porous structure as gas sensors are thought to not only provide a large number of channels for gas diffusion but also possess significantly large surface areas for gas-sensing reactions.[27,28] Moreover, the addition of V_2O_5 is supposed to improve the gas sensing performance of the composite. The synthesis process and experiment of raw

[a] College of Electrical and Information Engineering, Hunan University, China. Fax: +86 731 88664019; Tel: +86 731 88664019
[b] Pen-Tung Sah Institute of Micro-Nano Science and Technology of Xiamen University, Xiamen, 361005, China. E-mail: liqiuhong@xmu.edu.cn; Tel: 86-592-2187198
[c] Key Laboratory for Micro-Nano Optoelectronic Devices of Ministry of Education, School of Physics and Electronics, Hunan University, Changsha 410082, P. R. China
† Electronic supplementary information (ESI) available.
See DOI: 10.1039/x0xx00000x

materials are introduced in detail in the supplementary information.

X-ray diffraction (XRD) analysis was used to determine the crystal structure of the samples before and after soak-salcination. As shown in Fig. 1, all the reflection peaks of the sample before soak-salcination (the read line) can be indexed as standard α-Fe_2O_3 sample (Joint Committee on Powder Diffraction Standards (JCPDS) card no. 33-0664), which indicates that the sample synthesised by ES is α-Fe_2O_3. Moreover, the reflection peaks of the sample after soak-salcination (the black line) can be indexed as standard α-Fe_2O_3 sample (JCPDS card no. 33-0664) and standard V_2O_5 sample (JCPDS card no. 89-2482) demonstrating that through the soak-calcination strategy method, V_2O_5 nanoparticles were successfully synthesized in the composite.

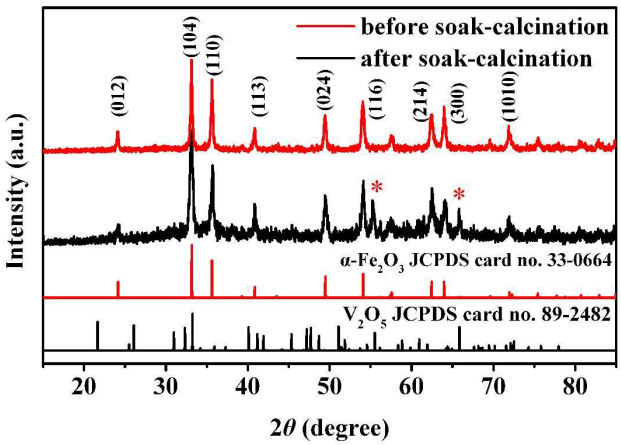

Fig. 1 XRD patterns of the samples before and after soak-salcination.

The morphologies of the as-prepared α-Fe_2O_3 nanorods and V_2O_5-decorated α-Fe_2O_3 nanorods were investigated based on the field-emission scanning electron microscopy (FE-SEM), transmission electron microscope (TEM) and element EDS mapping images shown in Fig. 2. Fig. 2a and b give a representative SEM image of the as-synthesized α-Fe_2O_3 nanorods, showing that the surface is smooth and uniform with diameters about 100 nm. Fig. 2c gives typical high magnification SEM images of the V_2O_5-decorated α-Fe_2O_3 nanorods showing that the surface is rougher than α-Fe_2O_3 nanorods (Fig. 2a) and are uniform with the diameters about 100 nm. The EDS spectrum of V_2O_5-decorated α-Fe_2O_3 nanorods from SEM certificated the presence and proportion of Fe, O and V (Fig. S1). TEM, high-resolution TEM (HRTEM) and the corresponding EDS elemental mapping images provide further insight into the microstructure and morphology of the product. Fig. 2d shows a typical TEM image of α-Fe_2O_3 nanorods. Structural information was further characterized by HRTEM in Fig. 2e. Lattice spacings of 0.2271 nm and 0.2710nm for the nanorods correspond to (113) and (024) plane of rhombohedral α-Fe_2O_3 (Fig. 1). TEM image (Fig. 2f and g) shows that V_2O_5 nanoparticles were modified on the surface of α-Fe_2O_3 nanorods. HRTEM (Fig. 2h) of the nanoparticle showed that lattice spacing of 0.2503 nm correspond to the (005) plane of rutile V_2O_5. Moreover, Fig. 2i shows element mapping of Fe, V and O in one single V_2O_5-decorated α-Fe_2O_3 nanorod. The results demonstrate that Fe, V and O are distributed throughout nanorods which confirm V_2O_5 nanoparticles were modified on the surface of α-Fe_2O_3 nanorods. In other words, through the soak-calcination strategy, V_2O_5 nanoparticles were successfully decorated on the α-Fe_2O_3 nanorods.

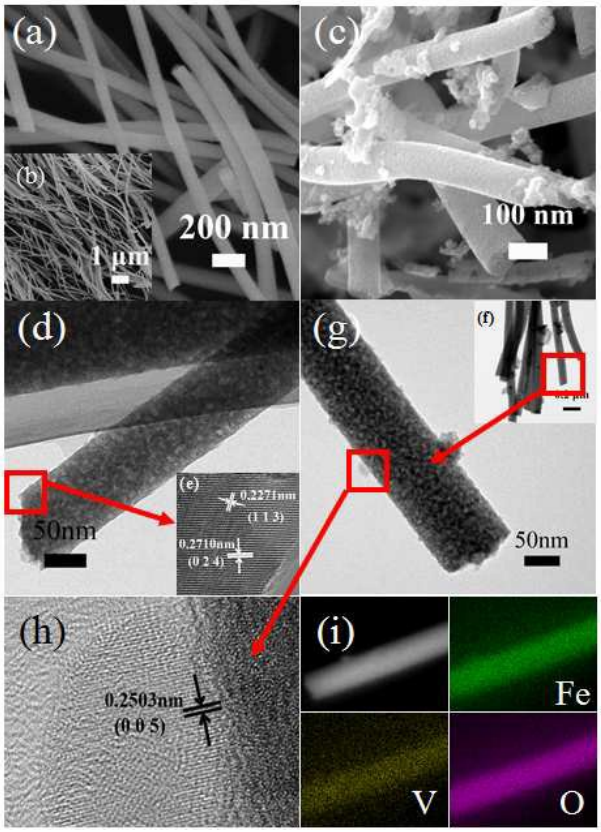

Fig. 2 SEM images of (a, b) α-Fe_2O_3 nanorods, (c) V_2O_5-decorated α-Fe_2O_3 composite nanorods. (d, e) and (f-h) TEM images of α-Fe_2O_3 nanorods and V_2O_5-decorated α-Fe_2O_3 composite nanorods respectively. (i) Elemental mapping images of Fe, V and O element.

The operating temperature is closely linked with the response for semiconductor oxide sensors. As shown in Fig 3a, the responses of three sensors to 100 ppm diethylamine were measured under different operating temperatures from 150 °C to 350 °C. Evidently, the sensitivity of the V_2O_5-decorated α-Fe_2O_3 nanorods increases with working temperature and reaches a maximum value of 8.9 at 350 °C. Because V_2O_5-decorated α-Fe_2O_3 nanorods were calcined at 350 °C for 2 h in air, the working temperature in this work was limited to 350°C. Similar tendencies are observed for the sensors based on α-Fe_2O_3 nanorods and c-V_2O_5, respectively. The maximum sensitivities of pure α-Fe_2O_3 nanorods is 2.97 at 250 °C and that of c-V_2O_5 is 1.63 at 200 °C, both of which are much smaller than that of V_2O_5-decorated α-Fe_2O_3 nanorods. According to the oxygen adsorption theory, when the operating temperature is low, physical adsorption is happened in general, when operating temperature is high there comes the chemical adsorption. Optimum operating temperature is related to

morphology, synthetic proces, environment conditions, etc. Although the optimum operating temperature was increased after combination of V_2O_5, sensitivity of the V_2O_5-decorated α-Fe_2O_3 composite is obviously higher than those of the pristine α-Fe_2O_3 nanorods and c-V_2O_5. Fig. 3b shows the sensitivity–concentration curves of the V_2O_5-decorated α-Fe_2O_3 nanorods, α-Fe_2O_3 nanorods and c-V_2O_5. α-Fe_2O_3 nanorods and c-V_2O_5 show sensitivities of approximately 1-3.2 and 1.1-1.9, to 5–300 ppm diethylamine, respectively. In contrast, V_2O_5/α-Fe_2O_3 nanorods show a sensitivity of about 1.8-9.5 to 5–300 ppm diethylamine. The sensitivity of the V_2O_5-decorated α-Fe_2O_3 nanorods is significantly increased with increasing diethylamine concentration, while the increase in the sensitivities of α-Fe_2O_3 nanorods and c-V_2O_5 is very little. These results indicate that for detecting diethylamine, the sensitivity of the V_2O_5-decorated α-Fe_2O_3 nanorods is obviously higher than those of the pristine α-Fe_2O_3 nanorods and c-V_2O_5. Fig. 3 c-e display the response of sensors to 100 ppm diethylamine at 350 °C. The response time is defined as the time taken for the sensor to achieve 90% of total resistance, and the recovery time is the time for the resistance to recover to 90% of the initial level after removal of diethylamine vapor. The response curve shows a drastic decline once the sensor is exposed to target gases and achieves a near steady state, then rises to its initial value in air. It can be observed that the three sensors display fast response/recovery time: 2 s/40 s (V_2O_5-decorated α-Fe_2O_3 nanorods), 14 s/1 s (α-Fe_2O_3 nanorods), and 9.5 s/40 s (c-V_2O_5) to 100 ppm diethylamine, respectively.

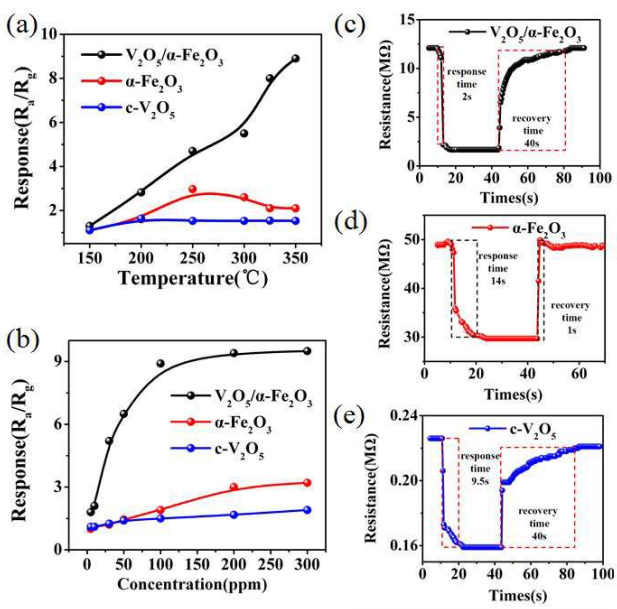

Fig. 3 (a) Response of sensor based on the V_2O_5-decorated α-Fe_2O_3 nanorods, α-Fe_2O_3 nanorods and commercial V_2O_5 (c-V_2O_5) sensors to 100 ppm diethylamine at different operating temperatures; (b) Response of the V_2O_5-decorated α-Fe_2O_3 nanorods, α-Fe_2O_3 nanorods and c-V_2O_5 sensors to 5–300 ppm of diethylamine at 350 °C; (c-e) response/ recovery curves of the V_2O_5-decorated α-Fe_2O_3 nanorods, α-Fe_2O_3 nanorods and c-V_2O_5 sensors to 100 ppm diethylamine at 350 °C.

The responses of the three sensors towards a variety of flammable, toxic gases including diethylamine, formaldehyde, n-hexane, trichloromethane, glycol, ammonium hydroxide, ethylenediamine, CH_4, CO and SO_2 are studied to evaluate the selectivity of the sensors. As shown in Fig. 4a, the responses of the V_2O_5-decorated α-Fe_2O_3 nanorods sensor to the ten gases are all improved compared with those of the α-Fe_2O_3 nanorods and c-V_2O_5. In addition, the sensor based on V_2O_5-decorated α-Fe_2O_3 nanorods shows superior sensitivity to diethylamine compared with other gases; the response is 3-8.1 times higher than those for the other tested gases, which indicates an excellent selectivity to diethylamine. Fig. 4b shows the responses of V_2O_5-decorated α-Fe_2O_3 nanorods, α-Fe_2O_3 nanorods and c-V_2O_5 sensors to 30ppm diethylamine at 350 ℃. In our practical gas sensor test, the resistance of α-Fe_2O_3 sensor in the air is not stable but regular. So we choose and calculate the average resistance of the sensor to calculate the response of it. As the resistance baseline of V_2O_5 is very stable, when the V_2O_5 was decorated on the surface of α-Fe_2O_3 nanorods, the sensor of V_2O_5-decorated α-Fe_2O_3 composite become stable because of the synergistic effect. The sensor of V_2O_5-decorated α-Fe_2O_3 nanorods demonstrates remarkable repeatability with outstanding stability campared with α-Fe_2O_3 nanorods sensor.

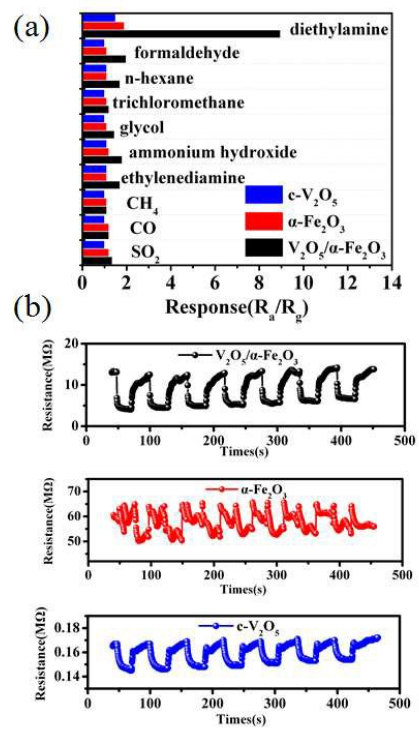

Fig. 4 (a) Selectivity tests to 100 ppm of different gases at 350 °C. (b) The response of V_2O_5-decorated α-Fe_2O_3 nanorods, α-Fe_2O_3 nanorods and c-V_2O_5 sensors to 30ppm diethylamine at 350 °C.

We confirmed this structure feature by N_2 adsorption-desorption measurements. As expected, the V_2O_5-decorated α-Fe_2O_3 composite shows a Brunauer-Emmett-Teller (BET) specific surface area of 30.5 m^2 g^{-1} with pore volume of 0.19

cm^3 g^{-1}, higher than α-Fe_2O_3 nanorods with specific surface area of 24.6 m^2 g^{-1} and pore volume of 0.077 cm^3 g^{-1} which is showed in Fig S3. The larger surface area could facilitate the absorption of gas molecule. Fig S4 shows the pore size distribution of V_2O_5-decorated α-Fe_2O_3 composite and α-Fe_2O_3 nanorods obtained from the desorption branch of the isotherm. With regard to α-Fe_2O_3 nanorods, there are numerous micropores around 1.6 nm and 1.8 nm, and the mesopores between 2 and 5 nm. After soak-calcination method, there are more micropores existed around 0.9 nm and mesopores between 2 and 10 nm. The high specific surface area and optimized pore structure are beneficial for absorption of gas molecule.

Based on the above results, the reason was discussed for the improvement in gas-sensing properties of α-Fe_2O_3 nanorods decorated with the V_2O_5 nanoparticles. It is well known that both Fe_2O_3 and V_2O_5 are n-type semiconducting oxides and their sensing mechanism is the surface-controlled type.[29,30] Their gas sensitivity depends on grain size, porosity, active surface state, oxygen adsorption quantity, active energy of adsorption of the test gas on the surface, lattice defect and so on. [31] According to the above FESEM and TEM analysis, it is observed that after being sintered, α-Fe_2O_3 nanorods with V_2O_5 nanoparticles form some pores in different sizes. Those pores with small diameters become closed gas pores in the sintering process, or move to the grain boundaries and gradually disappear, while those pores with larger diameters will shrink slightly, but will not disappear. The porous structure on the surface of the element not only provides enough space to reduce space hindrance induced by the gas adsorption, but also increases its inner surface, thus the gas can be adsorbed on the inner surface of the element through Van der Waals force. This could help to improve the gas adsorption and sensitivity. The amount of V_2O_5 in the α-Fe_2O_3 nanorods was calculated which is about 17% according to presence of Fe and V atom in the EDS of SEM (Fig. S1). As we know the presence of atom in EDS of SEM is inaccuracy with certain reference. The modification of metal oxides by additives or dopants is well-known for improving the performances of resulting chemoresistive gas sensors.[32,33] Additives may induce electronic sensitization, based on the modification of the electronic properties of the host oxide[34,35], or spillover[36-39]. Nanomaterials incorporated with V_2O_5 can significantly enhance the sensing performances in this paper and other literatures.[40,41] The sensing results showed that by introducing V in the α-Fe_2O_3 structure it was possible to obtain larger responses, shorter response time and much stable at appropriated temperatures, which is just the aim of surface modifications. In Fe_2O_3-V_2O_5, more effective diethylamine oxidation took place, while in pure α-Fe_2O_3 a reaction with lower activation energy was operative. In addition, the one-dimensional nanorods form a network in the V_2O_5-decorated α-Fe_2O_3 nanocomposite, which are favorable for conducting the charges induced when being exposed to the samples. As far as we know, there is no diethylamine gas sensing literature, the mechanism of why sensing selectivity enhanced by doping V_2O_5 may be as follows. Hence, it is reasonable to search for hints in catalysis field about how to improve chemoresistive sensors. A well-known catalyst system is the titania-supported vanadium pentoxide[42, 43]which is similar to our V_2O_5/α-Fe_2O_3 nanorods. Diethylamine gas is one of the volatile organic compounds (VOCs). Particularly, it is known as a promoter of oxidation reactions of many organic compounds[44,45], which makes it an ideal candidate for detection of volatile organic compounds.[46] As aforementioned, V_2O_5 nanoparticles significantly enhance the gas-sensing properties of α-Fe_2O_3 nanorods. More details of the enhancing effect of the V_2O_5 nanoparticles on the sensing properties of the Fe_2O_3 nanorods need further investigation.

Conclusions

In conclusion, V_2O_5-decorated α-Fe_2O_3 composite nanorods were synthesized successfully by electrospinning and environment-friendly soak-calcination method. The nanorods show high selectivity and outstanding stability to diethylamine gas as well as ultra fast response within 2s. The result provides a way to develop high-performance sensors by electrospinning and environment-friendly soak-calcination strategy, which can be explored to other sensitive materials.

Acknowledgements

This work was partly supported by the National Natural Science Foundation of China (Grant No. 61574118), the Specialized Research Fund for the Doctoral Program of Higher Education of China (20120161110016), and the Hunan Provincial Innovation Foundation for Postgraduates (Grant no. CX2014B133).

Notes and references

1 Z. J. Fan, J. Yan, L. J. Zhi, Q. Zhang, T. Wei, J. Feng, M. L. Zhang, W. Z. Qian and F. Wei, *Adv. Mater.*, 2010, **22**, 3723.
2 D. W. Wang, F. Li, J. P. Zhao, W. C. Ren, Z. G. Chen, J. Tan, Z. S. Wu, I. Gentle, G. Q. Lu and H. M. Cheng, *ACS Nano*, 2009, **3**, 1745.
3 L. Mei, Y. J. Chen and J. M. Ma, *Scientific Reports*, 2014, **4**, 6028.
4 Y. Q. Liang, Z. D. Cui, S. L. Zhu, Z. Y. Li, X. J. Yang, Y. J. Chen and J. M. Ma, *Nanoscale*, 2013, **5**, 10916.
5 L. Wang, Y. J. Chen, J. M. Ma, L. B. Chen, Z. Xu and T. H. Wang, *Scientific Reports*, 2013, **3**, 3500.
6 H. J. Kim, J. W. Yoon, K. I. Choi, H. W. Jang, A. Umarcd and J. H. Lee, *Nanoscale*, 2013, **5**, 7066.
7 J. Deng, J. Ma, L. Mei, Y. Tang, Y. Chen, T. Lv, Z. Xu and T. Wang, *J. Mater. Chem. A*, 2013, **1**, 12400.
8 G. Faglia, C. Baratto, G. Sberveglieri, M. Zha and A. Zappettini, *Appl. Phys. Lett.*, 2005, **86**, 011923.
9 G. Mattei, P. Mazzoldi, L. Post, M. D. Buso, M. Guglielmi and A. Martucci, *Adv. Mater.*, 2007, **19**, 561.
10 G. Korotcenkov, V. Brinzari, J. R. Stetter and I. Blinov and V. Blaja, *Sens. Actuators, B*, 2007, **128**, 51.
11 N. Tamaekong, C. Liewhiran, A. Wisitoraat and S. Phanichphant, *Sens. Actuators, B*, 2011, **152**, 155.
12 X. Y. Xue, L. L. Xing, Y. J. Chen, S. L. Shi, Y. G. Wang and T. H. Wang, *J. Phys. Chem. C* 2008, **112**, 12157.
13 L. C. Tien, P. W. Sadik, D. P. Norton, L. F. Voss, S. J. Pearton, H. T. Wang, B. S. Kang, F. Ren, J. Jun and J. Lin, *Appl. Phys.*

Lett.
2005, **87**, 222106.
14 A. Kolmakov, D. O. Kienov, Y. Liach, S. Stemmer and M. Moskovits, *Nano Lett.,* 2005, **5**, 667.
15 A. Katoch, S.-W. Choi, G.-J. Sun, H. W. Kim and S. S. Kim, *Nanotechnology*, 2014, **25**, 175501.
16 J. Wang, L. Wei, L. Zhang, J. Zhang, H. Wei, C. Jiang and Y. Zhang, *J. Mater. Chem.*, 2012, **22**, 20038.
17 D. Chen, J. Xu, Z. Xie and G. Z. Shen, *ACS Appl. Mater. Interfaces*, 2011, **3**, 2112.
18 N. Yamazoe, K. Suematsu and K. Shimanoe, *Sens. Actuators, B*, 2012, **163**, 128.
19 N. Yamazoe, K. Suematsu and K. Shimanoe, *Thin Solid Films*, 2013, **548**, 695.
20 M. H. Seo, M. Yuasa, T. Kida, J.-S. Huh, N. Yamazoe and K. Shimanoe, *Sens. Actuators, B*, 2011, **154**, 251.
21 Z. Wang, H. Yin, C. Jiang, M. Safdar and J. He, *Appl. Phys. Lett.*, 2012, **101**, 253109.
22 X. Tang, F.L. Yan, Y. H. Wei, M. Zhang, T. H. Wang and T. F. Zhang, *ACS Appl. Mater. Interfaces*, 2015, **7**, 21890.
23 X. L. Hu, J. C. Yu, J. M. Gong, Q. Li, and G.S. Li, *Adv. Mater.* 2007, **19**, 2324.
24 V. Petkov, P. N. Trikalitis, E. S. Bozin, S. J. L. Billinge, T. Vogt, and M. G. Kanatzidis, *J. Am. Chem. Soc.*, 2002, **124**, 10157.
25 H. S. Kim, C. H. Jin, S. H. Park and C. M. Lee, *J. Electroceram,* 2013, **30**, 6.
26 M. Epifani, R. Díaz, C. Force, E. Comini, T Andreu, R. R. Zamani, J Arbiol, P Siciliano, G Faglia and J. R. Morante, *J. Phys. Chem. C,* 2013, **117**, 20697
27 M. Ding, D. C. Sorescu and A. Star, *J. Am. Chem. Soc.*, 2013, **135**, 9015.
28 X. Sun, H. Ji, X. Li, S. Cai and C. Zheng, *J. Alloys Compd.*, 2014, **600**, 111.
29 J. Deng, J. Ma, L. Mei, Y. Tang, Y. Chen, T. Lv, Z. Xu and T. Wang, *J. Mater. Chem. A*, 2013, **1**, 12400.
30 Z. Dai, C. Lee, Y. Tian, Il. Kimb and J. Lee, *J. Mater. Chem. A*, 2015, **3**, 3372.
31 W. Zhang, W. Zhang, *Sens. Actuators, B*, 2008, **134**, 403.
32 G. Korotcenkov, *Sens. Actuators, B: Chem.* 2005, **107**, 209.
33 M. N. Rumyantseva, O. V. Safonova, M. N. Boulova and A. M. Gas'kov, *Russ.Chem. Bull.* 2003, **52**, 1217.
34 V. Dobrokhotov, D. N. McIlroy, M. G. Norton, L. Wang, *J. Appl. Phys.* 2006, **99**, 104302.
35 A. Kolmakov, D. O. Klenov, Y. Lilach, S. Stemmer, M. Moskovits, *Nano Lett.* 2005, **5**, 667.
36 W. C. Conner, J. L. Falconer, *Chem. Rev.* 1995, **95**, 759.
37 U. Heiz, E. L. Bullock, *J. Mater. Chem.* 2004, **14**, 564.
38 G. M. Pajonk, *Chem. Rev.* 1994, **1**, 329−338.
39 G. M. Pajonk, *Appl. Catal., A* 2000, **202**, 157−169.
40 H. S. Kim, C. H. Jin, S. H. Park and C. M. Lee, *J. Electroceram,* 2013, **30**, 6.
41 M. Epifani, R. Díaz, C. Force, E. Comini, T Andreu, and J. R. Morante, *J. Phys. Chem. C*, 2013, **117**, 20697.
42 J. Haber, *Catal. Today* 2009, **142**, 100.
43 B. M. Weckhuysen, D. E. Keller, *Catal. Today,* 2003, **78**, 25.
44 H. S. Kim, C. H. Jin, S. H. Park and C. M. Lee, *J. Electroceram,* 2013, **30**, 6.
45 A.Bruckner, M. Baerns, *Appl. Catal., A,* 1997, **157**, 311−334.
46 B. GrzybowskaSwierkosz, *Appl. Catal., A,* 1997, **157**, 263−310